

Mitochondria produce reactive nitrogen species via an arginine-independent pathway

ZSOMBOR LACZA^{1,2}, ANDREY V. KOZLOV³, ESZTER PANKOTAI², ATTILA CSORDÁS², GERALD WOLF⁴, HEINZ REDL³, MÁRK KOLLAI², CSABA SZABÓ², DAVID W. BUSIJA¹ & THOMAS F. W. HORN⁴

¹Department of Physiology/Pharmacology, Wake Forest University Health Sciences, Medical Center Blvd, Winston-Salem, NC 27157, USA, ²Institute of Human Physiology and Clinical Experimental Research, Semmelweis University, Üllői út 78/a, Budapest 1082, Hungary, ³Ludwig Boltzmann Institute for Experimental and Clinical Traumatology in the Research Center of AUVA, Donaueschingen strasse 13, Vienna A-1200, Austria, and ⁴Institute for Medical Neurobiology, Otto-von-Guericke University, Leipziger Street 44, Magdeburg D-39120, Germany

Accepted by Dr T. Grune

(Received 26 August 2005; in revised form 26 October 2005)

Abstract

We measured the contribution of mitochondrial nitric oxide synthase (mtNOS) and respiratory chain enzymes to reactive nitrogen species (RNS) production. Diaminofluorescein (DAF) was applied for the assessment of RNS production in isolated mouse brain, heart and liver mitochondria and also in a cultured neuroblastoma cell line by confocal microscopy and flow cytometry. Mitochondria produced RNS, which was inhibited by catalysts of peroxynitrite decomposition but not by nitric oxide (NO) synthase inhibitors. Disrupting the organelles or withdrawing respiratory substrates markedly reduced RNS production. Inhibition of complex I abolished the DAF signal, which was restored by complex II substrates. Inhibition of the respiratory complexes downstream from the ubiquinone/ubiquinol cycle or dissipating the proton gradient had no effect on DAF fluorescence. We conclude that mitochondria from brain, heart and liver are capable of significant RNS production via the respiratory chain rather than through an arginine-dependent mtNOS.

Keywords: DAF-2, DAF-FM, nitric oxide, nitric oxide synthase, NOS, ONOO⁻

Abbreviations: 3-NPA, 3-nitropropionic acid; DAF2-DA, 4,5-diaminofluorescein diacetate; DAF-FM, 4-amino-5-methylamino-2',7'-difluorofluorescein; DMEM, Dulbecco's Modified Eagles Medium; DMSO, dimethyl-sulfoxide; eNOS, endothelial nitric oxide synthase; FCCP, carbonyl cyanide 4-(trifluoromethoxy) phenylhydrazone; FeTPPS, 5,10,15,20-tetrakis (4-sulfonatophenyl) porphyrinato iron (III) chloride; FP15, tetrakis 2-triethylene glycol monomethyl ether (pyridil porphyrin (2-T(PEG3)PyP); iNOS, inducible nitric oxide synthase; L-NAME, L-nitroarginine-methyl-ester; L-N-monomethylarginine, L-N-methylarginine; mtNOS, mitochondrial nitric oxide synthase; nNOS, neuronal nitric oxide synthase; NO, nitric oxide

Introduction

It is well known that nitric oxide (NO) has several targets within the mitochondrion. It inhibits mitochondrial respiration through binding to respiratory chain enzymes, modulates mitochondrial ATP dependent K⁺ channels, regulates the maturation of the organelle and it is metabolized by cytochrome c

oxidase [1–4]. Thus, it is an intriguing concept that mitochondria themselves can produce NO in physiologically relevant concentrations.

The existence of a distinct mitochondrial nitric oxide synthase enzyme (mtNOS) is much debated [5–8]. The initial finding of mitochondrial NADPH diaphorase activity in basilar arteries, a marker of NO

Correspondence: Z. Lacza, Üllői út 78/a, Budapest H-1082, Hungary. Tel: 36 1 2100306. Fax: 36 1 3343162. E-mail: zlacza@mac.com

synthesis, was followed by several reports which suggested the presence of various NOS isoforms and also NO production within mitochondria [9–15]. However, some of these early observations were not reproducible by other laboratories and the question of the existence of mtNOS cannot be conclusively answered at this time [6,16–18].

We and other laboratories consistently observed that NO-sensitive fluorescent probes display distinct mitochondrial signals in various preparations [16,19–23]. Probes such as the diaminofluoresceins DAF-2 or DAF-FM were designed for fluorescent measurement of NO production [24]. These dyes react with NO to form a benzotriazole product, which results in more than a 100 fold fluorescence increase. Diaminofluoresceins have been widely used for monitoring NO production in various experimental settings both *in vitro* and *in vivo* [25–27]. Based on the prominent DAF fluorescence signals in mitochondria, it seems that mitochondria produce high amounts of NO. However, this is in sharp contrast to the generally very low or nonexistent NOS activity of the mitochondria, or the lack of reports that show such a rather high NO release from the organelles measured with other than the fluorescent methods [16–18]. Moreover, it was shown that DAF-2 is sensitive to peroxynitrite [28]. Since mitochondria are major sources of superoxide, diffusing NO of any source may find its reaction partner to form peroxynitrite that in turn yields the fluorescent DAF-product. Indeed, recent studies from our laboratory and that of others have shown that the DAF fluorescence is significantly higher when other oxidants, such as superoxide or ONOO⁻ are present [16,28–30]. Therefore, we hypothesized that the fluorescent conversion of DAF in mitochondria is not primarily due to the high amounts of NO produced by mtNOS, but rather a result of the dye's interaction with other nitrogen species. To investigate this hypothesis we first tested if a NOS-dependent arginine-to-citrulline conversion pathway contributes to the mitochondrial DAF fluorescence. Then, we assessed the involvement of selected elements of the mitochondrial respiratory chain in the generation of the fluorescent DAF product. For this purpose we performed experiments on isolated mouse brain, heart and liver mitochondria and also on a human neuroblastoma cell line.

Materials and methods

All procedures were approved by the local Animal Care and Use Committee.

Mitochondria preparation

Mitochondria were prepared from halothane anesthetized mouse brain, heart and liver using the discontinuous Percoll gradient method as described

previously [12]. Six to ten week-old male wild-type mice were used from the C57/BL6 strain (Jackson, Bar Harbor, ME). The mitochondria preparation obtained with this method had a high respiratory ratio (4.94 ± 0.46). Purity testing by Western blotting of mitochondrial and endoplasmic reticulum markers (cytochrome c oxidase and calreticulin, respectively) and electron micrographs were applied regularly to maintain comparability of the results [16,17,31].

Fluorescent confocal microscopy

Freshly isolated mitochondria were dispersed in K⁺-buffer containing 125 mM KCl, 2 mM K₂HPO₄, 5 mM MgCl₂, 10 mM HEPES, 10 μM EGTA at pH 7.0 and plated on poly-D-lysine coated coverslips. Mitochondria were energized by the addition of malate (5 mM) and K-glutamate (5 mM). The mitochondrial membrane potential sensitive dye MitoFluorRed was used to label mitochondria (1 μM, Molecular Probes, Eugene, OR; visualisation at: excitation: 543 nm, emission: >560 nm). RNS production was measured by 4-amino-5-methylamino-2',7'-difluorofluorescein (DAF-FM, 7 μM, Molecular Probes, Eugene, OR, visualisation at: excitation: 488 nm, emission: 505–530 nm) [16]. Both fluorophores were dissolved in dimethyl-sulfoxide (DMSO) as stock solutions and final DMSO content in the preparations was 0.2%. Visualisation of the used fluorochromes was achieved using a Zeiss scanning confocal microscope (Axiovert 100M) combined with transmission light microscopy (differential interference contrast optics, DIC). Background fluorescence was below the detection limit.

Electron microscopy

Freshly isolated mitochondria samples were fixed for 3 h in 4% paraformaldehyde/0.05% glutaraldehyde in pH 7.4 phosphate buffer. The samples were embedded in LR-white, sectioned and collected on uncoated nickel grids. The sections were stained with osmium and observed and photographed using standard electron microscopy procedures.

Flow cytometry

Freshly isolated mitochondria were dispersed in K⁺ buffer containing mitochondrial substrates (see above, mitochondrial suspension dilution: 1:100 v/v) and the preparations were incubated for 20 min at 37°C to energize the mitochondria. Treatments were also added to the preparations at the beginning of the incubation. Following energization, DAF-FM (7 μM) was added to the preparations and the fluorescence was measured with flow cytometry. Forward-scatter, side-scatter and green fluorescence (FL1-H) were recorded by a BD-FacsCalibur flow

cytometer from 100,000 events in each preparation. Data were evaluated by the CellQuestPro software. Special care was taken to keep the preparations and the dyes in darkness throughout the experiment to avoid photoactivation of the fluorescent probe [32]. Experiments were performed in parallel in brain, heart and liver mitochondria and were reproduced at least two times. Mitochondrial fluorescence was observed under control conditions and in the presence of ONOO⁻ scavengers tetrakis 2-triethylene glycol monomethyl ether (pyridil porphyrin (2-T(PEG3)-PyP) (FP15, 100 μM, Inotek Corp, Beverly, MA) [33,34] or 5,10,15,20-tetrakis (4-sulfonatophenyl) porphyrinato iron (III) chloride (FeTPPS, 100 μM; Calbiochem, San Diego, CA). The contribution of the hypothetical mtNOS to the NO production detected by DAF was tested by supplementation of the K⁺ buffer with L-arginine (1 mM) and Ca²⁺ (1 μM) in the absence of EGTA, or in the presence or absence of the NOS inhibitor L-nitroarginine-methyl-ester (L-NAME, 1 mM) or L-N-methylarginine (L-NMMA, 1 mM). The following treatments and their combinations were used to test the involvement of the mitochondrial respiratory chain: the complex I blocker rotenone (10 μM) in the absence of mitochondrial substrates malate and glutamate or in the presence of K-succinate (5 mM); the succinate dehydrogenase (complex II) inhibitor 3-nitropropionic acid (3-NPA, 100 μM); the complex III inhibitor myxothiazole (10 μM), the complex IV inhibitor KCN (100 μM) and the protonophore carbonyl cyanide 4-(trifluoromethoxy) phenylhydrazone (FCCP, 10 μM). FCCP was dissolved in ethanol and the final ethanol content in the preparation was 1%. All other drugs were dissolved in H₂O and diluted to the final concentration with K⁺ buffer. Each compound was purchased from Sigma (St Louis, MO) unless otherwise stated.

Electron paramagnetic resonance (EPR) measurements

Mouse heart mitochondria were suspended in a buffer containing 105 mM KCl, 20 mM TRIS-HCl, 1 mM diethylenetriaminepentaacetic acid, 4 mM KH₂PO₄ and 1 mg/ml fatty acid-free bovine serum albumin (pH 7.4, 25°C). The final concentration of mitochondria was 0.5 mg of mitochondrial protein/ml. The mitochondria were stimulated by the addition of 10 mM succinate. The rate of ROS-RNS generation in heart mitochondria was detected in the presence of 250 μM of 1-hydroxy-3-carboxypyrrolidine (CPH) (Noxygen GmbH, Germany) as described previously [35]. Mitochondria were incubated for 20 min at 22 ± 1.5°C. The diffusion of oxygen was facilitated using a shaking table to provide gentle mixing of the mitochondrial suspension with air. Following incubation, the samples were placed in glass capillars and EPR spectra were recorded with an X-band MiniScope

200 EPR spectrometer, (Magnettech Ltd, Berlin, Germany). The general settings were: modulation frequency 100 kHz, modulation amplitude 2.5 G; gain 700, power 5 mW. Upon reaction with ROS or RNS CP-H is transformed into a stable CP' radical (3-carboxy-proxyl). Therefore, standard solutions of 3-CP were used to construct a calibration curve.

Cell culture

All cell culture chemicals were purchased from Gibco/Invitrogen, Karlsruhe, Germany. Human neuroblastoma cells (SH-SY5Y, DMSMZ, Germany, ACC-No. 209) were grown in Dulbecco's Modified Eagles Medium (DMEM, supplemented with 20% fetal calf serum, 1% L-glutamine and 0.1% penicillin/streptomycin mixture). The cells were harvested and seeded at a density of 1 × 10⁵ on 22 mm-glass coverslips coated with poly-D-lysine that were placed in six-well plates. After two days *in vitro*, the subconfluent cells were loaded with 7 μM 4,5-diaminofluorescein diacetate (DAF2-DA, Molecular Probes, Eugene, OR) and MitoTrackerCMTMRos (0.5 μM, Molecular Probes, Eugene, OR) in the medium simultaneously for 30 min. DAF-2-DA, 7 μM, was used for loading in cell cultures and DAF-FM in isolated mitochondria preparations, since the latter lack the necessary esterase activity to cleave the diacetate from DAF-DA to yield the free probe DAF-2. In organelle-free solutions, both DAF-2 and DAF-FM showed similar sensitivity to various NO donors (not shown). Therefore, we use the acronym DAF fluorescence for both DAF-2 and DAF-FM fluorescence throughout the manuscript.

Subsequently to the cell loading, the coverslips were mounted into an Attofluor (Molecular Probes, Leiden, Netherlands) perfusion chamber and inserted in the heated stage of a confocal microscope (37°C, Zeiss LSM Pascal on an Axiovert 100M, Göttingen, Germany). After washing the cultures with HBSS (in g/l: NaCl 8.006; KCl 0.373; CaCl₂ 0.205; glucose 0.991; Hepes 4.76; KH₂PO₄ 0.081; K₂HPO₄ 0.01045; NaHCO 0.840; MgCl₂ 0.182; pH 7.4 at 37°C) the fluorescence was recorded using a 63 × PlanApochromat lens (DAF: excitation at 488 nm, emission at 505–530 nm; MitoTrackerRed: excitation 543 nm, emission at > 560 nm). The images were obtained in the multitracking mode to avoid the overlap of the emission curves. Images were merged using the Zeiss LSM software.

Results

Localization of DAF-fluorescence to mitochondria

Using isolated mitochondria we observed a strong DAF fluorescence in confocal microscopic images (Figure 1). Interestingly, the intensity of fluorescence

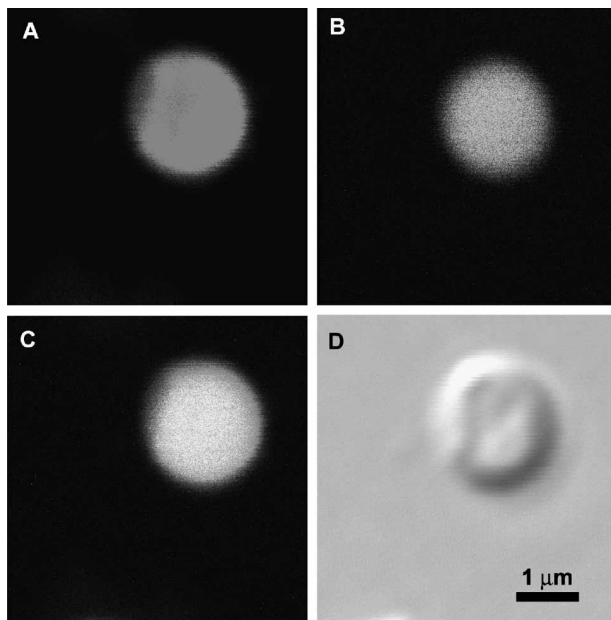


Figure 1. Mitochondrial localization of DAF fluorescence. Isolated respiring heart mitochondria were co-loaded with DAF-FM and MitoTrackerRed for 5 min and visualized by confocal microscopy. Panel A shows the MitoTrackerRed fluorescence. Note that the organelle has taken up the membrane potential sensitive dye, indicating intact respiration. Panel B shows that the green fluorescent DAF-FM is accumulated within a mitochondrion. Panel C shows the merged image, while Panel D is an image in transmitted light (DIC mode).

varied greatly among individual mitochondria even within the same preparation. To achieve consistent results, the subsequent experiments were conducted by flow cytometry, which allowed the quantitation of the fluorescence values of thousands of mitochondria from the same preparation. Each experiment was repeated at least two times, and variations among different preparations were minimal. Isolated mitochondria were depicted in a side-scatter–forward-scatter plot.

The autofluorescence of the mitochondrial flavoproteins was two orders of magnitude below that of mitochondria loaded with DAF (3 ± 4 vs 203 ± 196 ; Figure 2).

Comparisons between mitochondria obtained from tissues of different organs

Each experiment was performed in brain, heart and liver mitochondria preparations to investigate possible tissue-specific differences in mitochondrial RNS production. As seen in Figure 3, the side- and forward-scatter data from flow cytometry varies among the three regions; most notably the liver data extend to higher values than those of the heart or brain. Electron micrographs showed liver mitochondria to be round with a rosetta-like shape, while heart mitochondria are larger with very tight parallel cristae. Brain mitochondria were the most variable in size and shape with both elongated and round forms. However, the DAF fluorescence levels in the flow cytometry analysis were very similar in mitochondria of all three regions under baseline conditions. Also, in the presence of the various applied treatments the responses did not differ among mitochondria obtained from different tissues. Therefore, only data from heart mitochondria are shown below to avoid redundant figures. Comparisons were made only between preparations from the same animal and the same region and not between different experiments to exclude interpreparation variability.

Lack of contribution from the arginine-to-citrulline pathway to the mitochondrial DAF fluorescence

Isolated respiring mitochondria showed a similarly strong DAF fluorescence regardless of the presence or absence of the NOS substrate L-arginine or modulation of Ca^{2+} levels, the obligatory cofactor of NOS

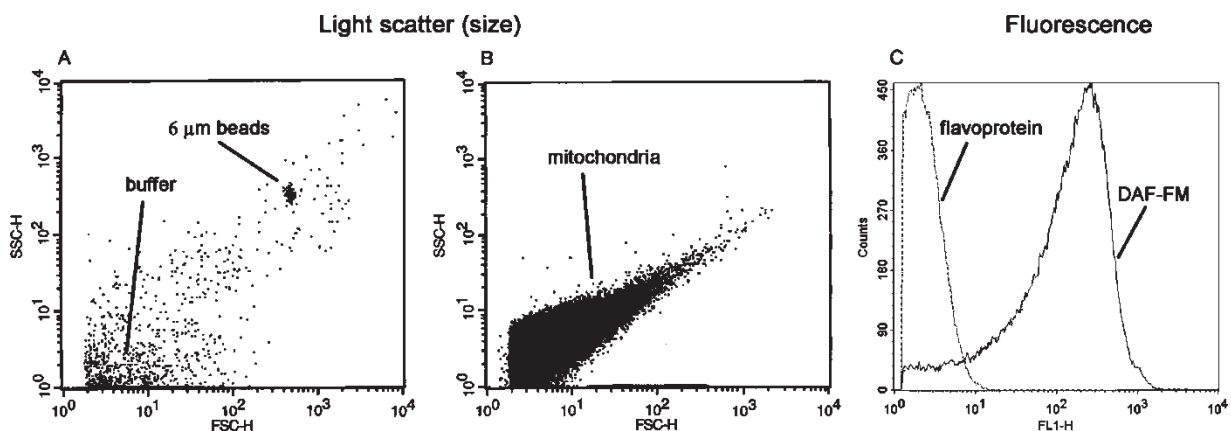


Figure 2. Investigation of isolated mitochondria with flow cytometry. Panel A shows the scatterplot of $6 \mu\text{m}$ fluorescein labeled beads in mitochondria-free buffer. As seen in Panel B, the majority of isolated heart mitochondria fall between the scatter plot coordinates of the beads and the buffer noise on Panel A. Panel C shows a fluorescence histogram of mitochondria in the absence and presence of DAF-FM to indicate background fluorescence. Autofluorescence of the mitochondrial flavoproteins was two orders of magnitude lower than the DAF fluorescence.

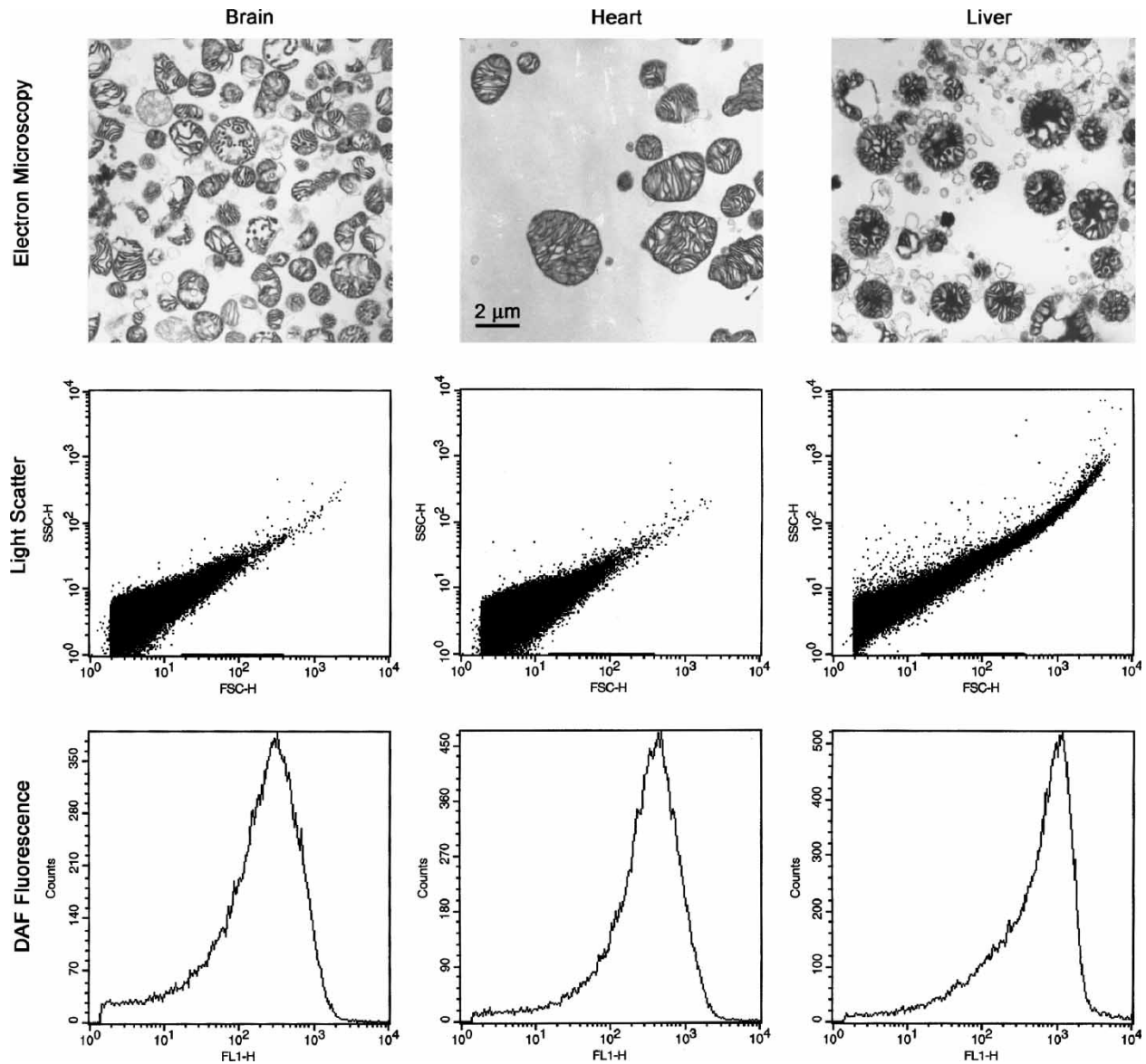


Figure 3. Comparative morphology and flow cytometric assessment of DAF-loaded mitochondria obtained from different tissues. The top row shows representative electron microscopic images of mitochondria isolated from mouse brain, heart and liver. Marked differences in size, shape and cristae formation can be observed among the regions and also within preparations. The middle row shows forward scatter-side scatter (FSC-H-SSC-H) plots of mitochondria recorded with flow cytometry. While brain and heart mitochondria have similar light scatter values, liver preparations are typically more spread out on the scatterplot, probably due to the tendency of liver mitochondria to stick together. The lower row shows DAF fluorescence histograms of the same preparations. Despite the apparent differences in morphology and light scatter, the different organ mitochondria have a similar DAF fluorescence profile.

(Figure 4). Blockade of a potentially mitochondrial-localized NOS by the competitive inhibitors L-NAME and L-NMMA failed to reduce mitochondrial DAF fluorescence (Figure 4). Prolonged *in vivo* application of L-NAME in the drinking water of the animals (10 mg/ml for 3 days) and supplementation of the mitochondria isolation buffers with L-NAME also failed to inhibit DAF fluorescence, making it very unlikely that the hypothetical mtNOS is responsible for the RNS production (Figure 4).

Addition of ONOO⁻ decomposition catalysts FeTPPS or FP15 to the mitochondria markedly decreased the fluorescence. Application of an SOD

mimetic (M40401) or catalase or the coapplication of both failed to affect the fluorescent signal, indicating that the DAF-FM fluorescence in mitochondria is not due to superoxide or hydrogen-peroxide but rather dependent on a nitrogen species such as ONOO⁻. These experiments confirmed that mitochondria produce RNS independently from the L-arginine-NOS pathway or reactive oxygen species.

Mitochondrial RNS production was also evaluated by the application of the spin trap CPH followed by electron spin resonance measurements. As seen on Figure 5, respiring mitochondria produced a significant amount of reactive species as shown using spin

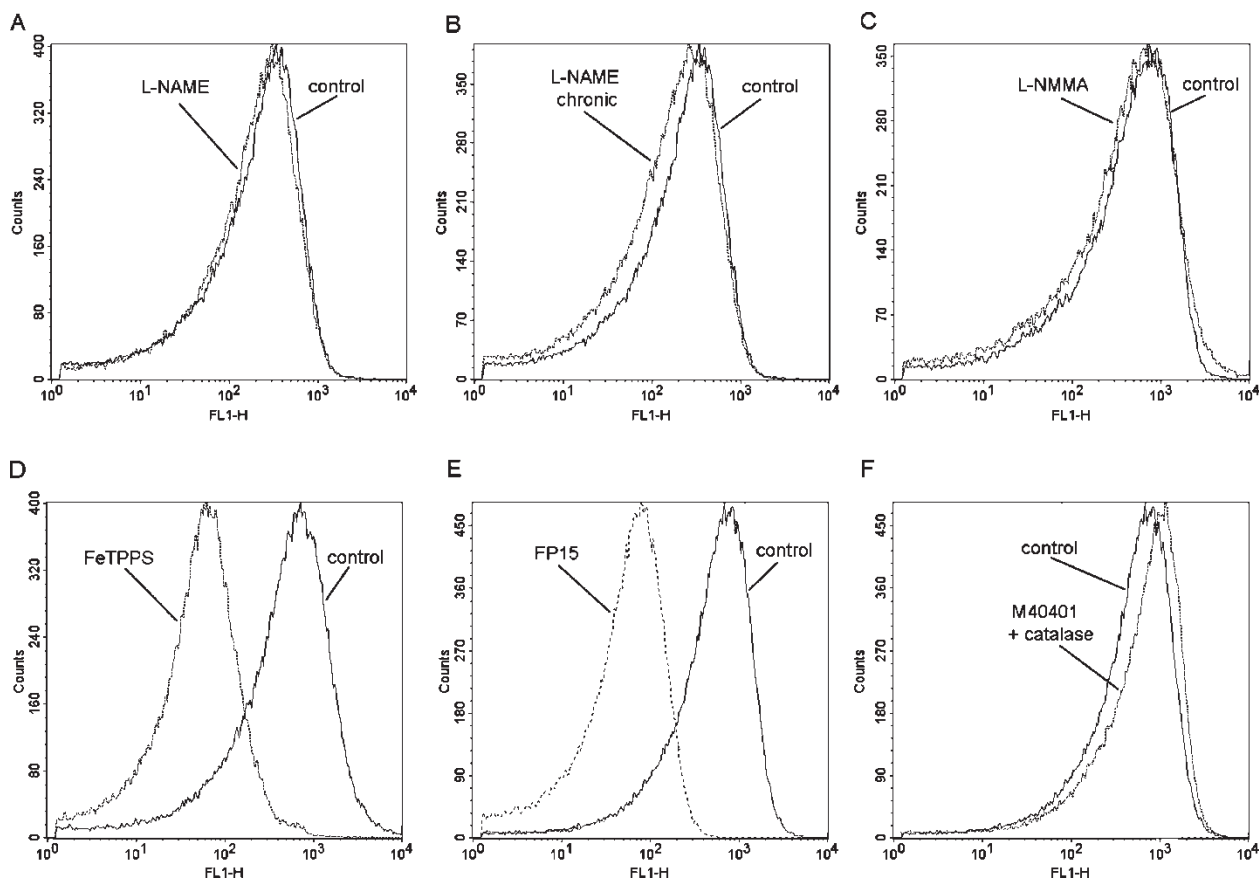


Figure 4. The role of reactive oxygen and nitrogen species in the generation of DAF fluorescence. Control measurements were performed under conditions favorable for NOS activity, i.e. supplementation of the K^+ buffer with L-arginine (1 mM) and Ca^{2+} (1 μ M) and the omission of EGTA. The pharmacological substances were added to the heart mitochondria preparations before they were incubated with DAF. Panels A, B and C show that the NOS inhibitors L-NAME and L-NMMA in the absence of arginine and Ca^{2+} fail to prevent the occurrence of the mitochondrial DAF fluorescence signal. In case of L-NAME, even prolonged application for three days in the drinking water (Panel B, “chronic L-NAME”) did not result in a reduced DAF signal. Panels D and E show that the presence of the ONOO⁻ decomposition catalysts FeTPPS and FP15 markedly inhibit DAF fluorescence. In contrast, Panel F shows that coapplication of an SOD mimetic (MK40401) and catalase does not affect the RNS production.

trapping technique. The generation of reactive species observed in this experiment was not sensitive to NO synthase inhibitors, complementing the data gathered by DAF fluorescence. Since the presence of SOD mimetics or ONOO⁻ decomposition catalysts in the reaction mixture interferes with the ESR measurements, the following experiments were carried out by flow cytometric quantitation of DAF fluorescence.

The involvement of the respiratory chain in mitochondrial RNS production

Mitochondrial DAF fluorescence was markedly inhibited when the organelles were denatured by three cycles of freezing and thawing or heating the preparations to 95°C for 5 min prior to the measurements (Figure 6). Similarly, DAF fluorescence was reduced when mitochondrial respiration was blocked by the application of rotenone or when respiratory

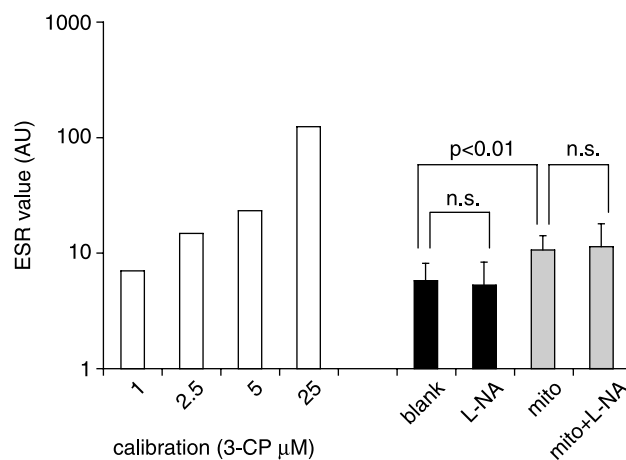


Figure 5. Measurement of mitochondrial reactive species production by EPR. Calibration data were obtained in mitochondria-free buffers containing increasing concentrations of the probe 3-CP. Live respiring heart mitochondria produced significant amounts of reactive species, which was not inhibitable by the presence of the NOS inhibitor L-NA.

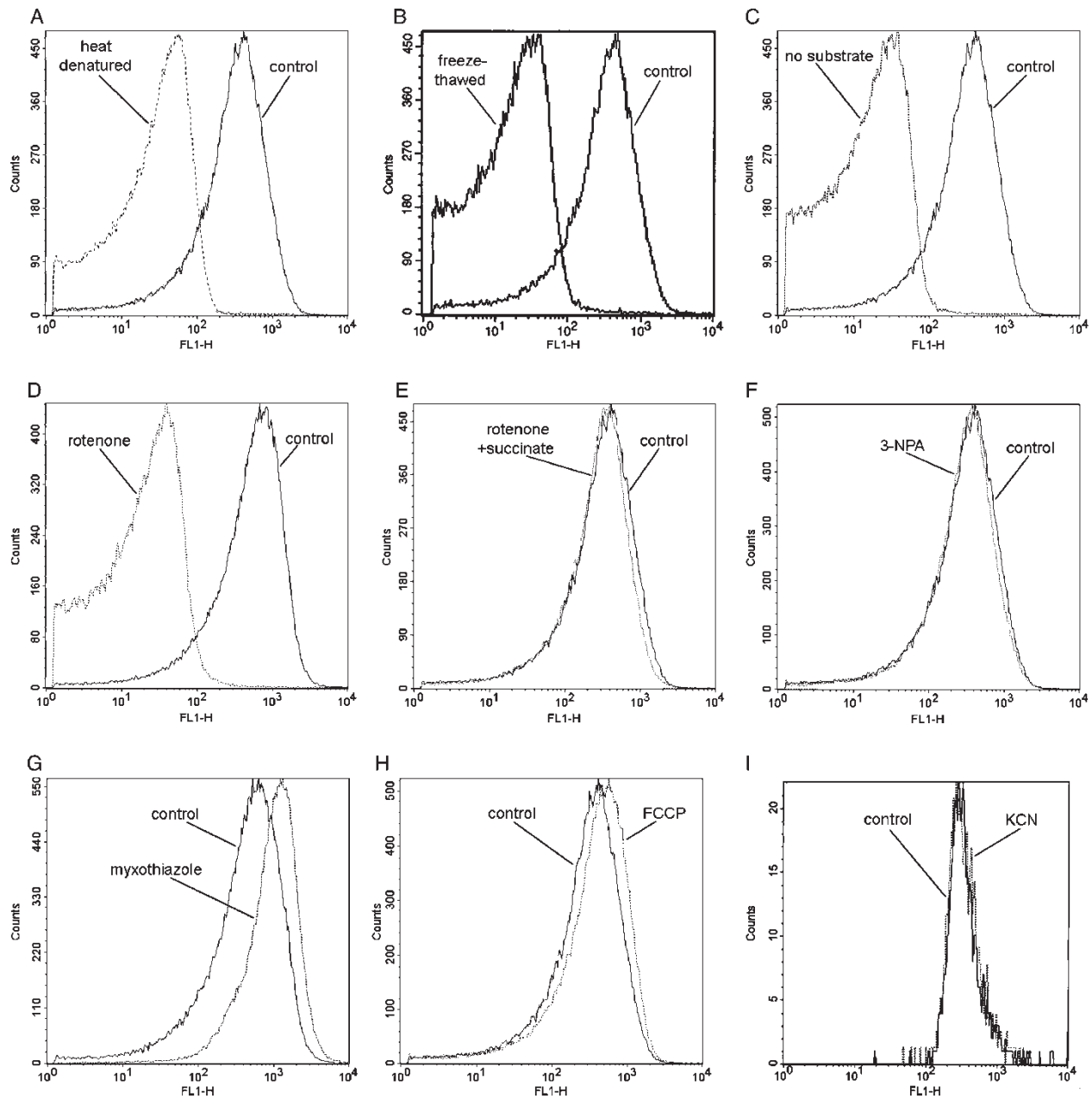


Figure 6. The role of the respiratory chain in generation of heart mitochondrial DAF fluorescence. The pharmacological substances were added to the preparations before addition of the fluorescent probe. Panels A and B show that deenergizing the mitochondria by physical disruption (boiling for 5 min at 95°C or three cycles of freezing and thawing) prevents the fluorescent conversion of DAF. Similar results can be obtained when the mitochondria do not receive any respiratory substrates (omission of malate and glutamate, Panel C) or when respiration is blocked by rotenone (Panel D). Panel E shows that respiration through complex I in the presence of glutamate and malate (control, Panel E) is equally effective as respiration through complex II in the presence of rotenone and succinate (Panel E). Panel F shows that the application of the succinate dehydrogenase inhibitor 3-NPA in the presence of glutamate and malate fails to decrease the fluorescence. Disrupting the transmembrane proton gradient by FCCP or inhibiting cytochrome c oxidase by KCN also leaves RNS production unaffected (Panels H and I). However, myxothiazole, an inhibitor of the ubiquinone oxidation site of complex III slightly increases DAF fluorescence (Panel G).

substrates malate and glutamate (5 mM each) were not supplemented in the medium (Figure 6). Inhibition of complex II by 3-NPA (100 μM) in the presence of complex I substrates malate and glutamate, or mitochondria respiring on succinate in the presence of the complex I inhibitor rotenone (5 mM and 10 μM , respectively) had similar fluorescence values, indicating that either complex I or complex II can

supply electrons for the reaction (Figure 6). Inhibition of the ubiquinone oxidation site of complex III with myxothiazole (10 μM) slightly increased the fluorescence, supporting that the ubiquinone pool is necessary for the reaction (Figure 6). Inhibition of complex IV by cyanide (100 μM) or collapsing the proton gradient by FCCP (10 μM) had no effect on RNS production (Figure 6).

Live cell imaging of DAF and MitoTracker fluorescence

We extended our investigations to live cells in order to exclude the possibility of preparation artifacts, which may arise in the artificial environment of isolated respiring mitochondria. Neuroblastoma SH5Y-5Y cells were imaged by confocal microscopy in a similar manner to that applied to isolated mitochondria. We observed a strong DAF fluorescence, which was completely co-localized with the mitotracker signal (Figure 7). DAF fluorescence was also prominent in the presence of the NOS inhibitor L-NAME or the protonophore FCCP (Figure 7), confirming the results obtained from isolated mitochondria.

Discussion

The main observation of the present study is that mitochondria produce RNS independently from the classical arginine-to-citrulline conversion pathway. The exact site of RNS production remains unknown, although electron transfer in the ubiquinone cycle of the respiratory chain is an obligatory step in the reaction. Such mitochondrial RNS production can be observed in all tested tissue types and, therefore, may be a common feature of all mitochondria.

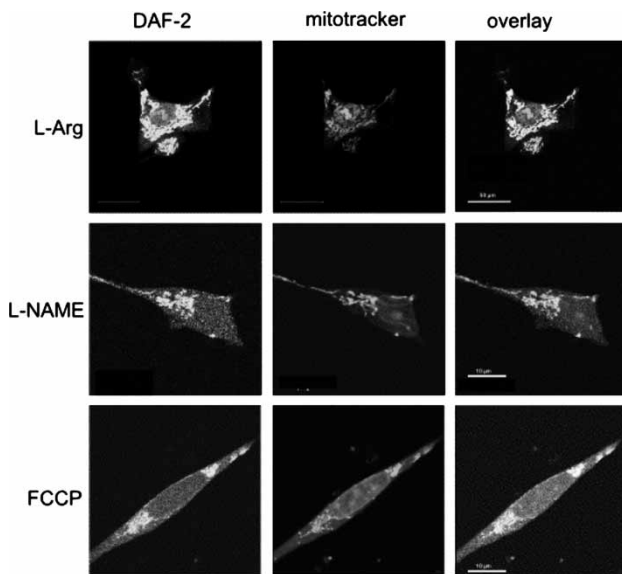


Figure 7. DAF-2 fluorescence in mitochondria of living neuroblastoma cells is independent of arginine or the mitochondrial proton gradient. Shown are representative images of neuroblastoma cells loaded with DAF-2-DA and MitoTrackerRed. The cells were first loaded with MitoTrackerCMTMRos for 30 min to label mitochondria. Subsequently, the medium was supplemented with either L-arginine (100 μ M, L-Arg), L-NAME (200 μ M) or FCCP (3 μ M) and all cultures were then incubated with DAF for 30 min. A distinct fluorescence of DAF was observed in the L-Arg treated cells that colocalized with the mitotracker signal. Neither L-NAME nor FCCP prevented the occurrence of mitochondrial DAF fluorescence.

These observations add a new aspect to the speculation regarding the existence of a mitochondrial RNS source by demonstrating an alternative pathway to the previously suggested mitochondrial NOS isoform [15,36]. In earlier studies, we and other laboratories investigated mitochondrial NO production with methods that were optimized for assessing the known NOS isoforms, such as measuring enzyme activity by the arginine to citrulline conversion assay or immunodetection of the enzyme protein with anti-NOS antibodies [11,12,36–39]. In some cases these methods yielded a very low signal, and concerns regarding the purity of the preparations added to the difficulty of interpreting the data. Recent studies described that the endothelial isoform of NOS can selectively bind to the outer mitochondrial membrane, which may account for the divergent data described in earlier studies to some degree [40,41].

In the present investigation, we focused on mitochondrial RNS production, which can be monitored using fluorescent probes. Several groups have found that the fluorescent DAF product accumulates in mitochondria of various origins [16,19–23]. We also showed that such DAF fluorescence is unaffected by the genetic disruption of nNOS, eNOS or iNOS, making it unlikely that NO produced by any of the known NOS isoforms contributes to the fluorogenic reaction [16,17]. Moreover, in the present paper, we show that mitochondrial DAF fluorescence cannot be reduced even by rather high concentrations or prolonged application of NOS blockers (1 mM L-NAME or L-NMMA, up to 3 days prior to the experiments in the drinking water of the animals). Withdrawal of L-arginine and Ca^{++} also failed to decrease DAF fluorescence in mitochondrial preparations, further supporting the idea that no arginine-dependent NOS is involved in the reaction.

The question arises whether it is possible that mitochondrial superoxide or other species react with the probe. The specificity of DAF to NO was extensively tested under *in vitro* conditions and it was shown that oxygen radicals alone are not capable of transforming the dyes into the fluorescent triazole products [24,42]. However, several investigators found that in living preparations, where a mixture of oxidants is present, DAF yields a much higher signal than NO can account for [16,28–30]. In the present study, we show that an coapplication of catalase and an SOD mimetic failed to alter the strong DAF signal in isolated mitochondria. However, two different ONOO⁻ decomposition catalysts (FP15 and FeTPPS) prevented DAF fluorescence, narrowing down the possible reactants with the probe to ONOO⁻. Nohl et al. suggest a pathway that may also lead from nitrite directly to ONOO⁻ [43]. Therefore, one may consider that the DAF fluorescence reflects RNS production in general, most possibly that of ONOO⁻ or one of its metabolites. Other methods, such as the hemoglobin

oxidation assay were also used for the quantitation of NO in mitochondria, however, this technique was shown to react with other N, O species just as the fluorescent probe used in the present study [44]. In any case, if within the vicinity of mitochondria any source of NO exists then part of such NO will diffuse into mitochondria and immediately form ONOO⁻ through the reaction with superoxide. This may account for the selective labeling of mitochondria by DAF fluorescence.

The integrity of the mitochondrion relies on the action of the respiratory chain, which produces ATP, utilizes O₂ and maintains the transmembrane electrochemical gradient. Denaturing the mitochondria by physically disrupting the organelle by heat or repeated freeze-thaw cycles successfully prevented DAF fluorescence. Inhibiting respiration by the lack of substrate has an effect similar to denaturing the organelles. Selective blockade of complex I inhibits mitochondrial RNS production, which can be reversed by the addition of succinate, a complex II substrate. Conversely, inhibition of complex II in the presence of complex I substrates fails to prevent RNS production. Blocking the respiratory chain downstream of the ubiquinone pool did not affect DAF fluorescence. Myxothiazole, which inhibits the ubiquinone oxidation site of complex III even increases the mean DAF fluorescence to some extent, supporting the idea that the ubiquinone pool is necessary for RNS production. Unexpectedly, even the disruption of the membrane potential by the protonophore FCCP leaves mitochondrial DAF fluorescence intact in both isolated mitochondria as well as in the whole cell approach. Summarizing the experiments with respiratory chain inhibitors it is clear that electron transport through complexes I and II to the ubiquinone cycle is necessary for RNS production, however, the lack of a proton gradient or ATP production does not affect it.

We conclude that mitochondria from brain, heart and liver tissues generate RNS to a similar extent via a mechanism independent from the arginine-to-citrulline conversion pathway. In other words, mitochondria act like nonspecific NO donors such as nitroprusside. What can be the source of NO and RNS in the mitochondrion? For example, it is possible that mitochondria take up NO from other sources and store it in the form of nitrosothiols. Such nitrosothiols can be found in mitochondria and act as NO donors [45]. Alternatively, mitochondria can convert organic nitrates into biologically active nitrogen species as was described previously [46,47]. Yet another possibility is that mitochondria convert nitrate to NO [9,43]. The production or the release of RNS from mitochondria can be blocked by inhibiting electron flow through the ubiquinone cycle. These results can be explained in three ways: RNS production responds to (1) electron flow itself, (2) an increase of reactive oxygen species (ROS) or (3) the redox state of the respiratory chain

(especially ubiquinones). Among these three possibilities, an influence of electron flow seems to be unlikely, because such flow should have stopped in all cases. Involvement of ROS also seems to be a remote possibility, since KCN is known to produce very little ROS. Therefore, the redox state of the respiratory chain (especially ubiquinones) might be the most feasible explanation.

Acknowledgements

The authors are grateful to Ken Grant for his invaluable help with confocal and electron microscopy and Dr Martha Alexander-Miller for her suggestions on flow cytometry. This study was supported by grants from the American Heart Association (Mid-Atlantic Grant 99512724, Bugher Foundation Award 0270114N) and the NIH (HL30260, HL46558, HL50587, HD38964); the Hungarian OTKA (D-45933, K-49621, AT-49488, T-47095), ETT (248/2003, 249/2003) and GVOP (TST 0002/2004); T.H. and G.W. are supported by grants SA 3521B/0703M and NBL3/PFG 01770407.

References

- [1] Brown GC. Nitric oxide and mitochondrial respiration. *Biochim Biophys Acta* 1999;1411:351–369.
- [2] Almeida A, Bolanos JP, Medina JM. Nitric oxide mediates brain mitochondrial maturation immediately after birth. *FEBS Lett* 1999;452:290–294.
- [3] Boveris A, Costa LE, Poderoso JJ, Carreras MC, Cadenas E. Regulation of mitochondrial respiration by oxygen and nitric oxide. *Ann NY Acad Sci* 2000;899:121–135.
- [4] Pearce LL, Kanai AJ, Birder LA, Pitt BR, Peterson J. The catabolic fate of nitric oxide: The nitric oxide oxidase and peroxynitrite reductase activities of cytochrome oxidase. *J Biol Chem* 2002;277:13556–13562.
- [5] Brookes PS. Mitochondrial nitric oxide synthase. *Mitochondrion* 2004;3:187–204.
- [6] Lacza Z, Pankotai E, Csordas A, Gero D, Kiss L, Horvath EM, Kollai M, Busija DW, Szabo C. Mitochondrial NO and reactive nitrogen species production: Does mtNOS exist? *Nitric Oxide* 2005;
- [7] Ghafourifar P, Cadenas E. Mitochondrial nitric oxide synthase. *Trends Pharmacol Sci* 2005;26:190–195.
- [8] Haynes V, Elfering S, Traaseth N, Giulivi C. Mitochondrial nitric-oxide synthase: Enzyme expression, characterization, and regulation. *J Bioenerg Biomembr* 2004;36:341–346.
- [9] Kozlov AV, Staniek K, Nohl H. Nitrite reductase activity is a novel function of mammalian mitochondria. *FEBS Lett* 1999;454:127–130.
- [10] Loesch A, Belai A, Burnstock G. An ultrastructural study of NADPH-diaphorase and nitric oxide synthase in the perivascular nerves and vascular endothelium of the rat basilar artery. *J Neurocytol* 1994;23:49–59.
- [11] Ghafourifar P, Richter C. Nitric oxide synthase activity in mitochondria. *FEBS Lett* 1997;418:291–296.
- [12] Lacza Z, Puskar M, Figueroa JP, Zhang J, Rajapakse N, Busija DW. Mitochondrial nitric oxide synthase is constitutively active and is functionally upregulated in hypoxia. *Free Radic Biol Med* 2001;31:1609–1615.
- [13] Bates TE, Loesch A, Burnstock G, Clark JB. Mitochondrial nitric oxide synthase: A ubiquitous regulator of oxidative

- phosphorylation? *Biochem Biophys Res Commun* 1996;218:40–44.
- [14] Bates TE, Loesch A, Burnstock G, Clark JB. Immunocytochemical evidence for a mitochondrially located nitric oxide synthase in brain and liver. *Biochem Biophys Res Commun* 1995;213:896–900.
- [15] Giulivi C, Poderoso JJ, Boveris A. Production of nitric oxide by mitochondria. *J Biol Chem* 1998;273:11038–11043.
- [16] Lacza Z, Snipes JA, Zhang J, Horvath EM, Figueroa JP, Szabo C, Busija DW. Mitochondrial nitric oxide synthase is not eNOS, nNOS or iNOS. *Free Radic Biol Med* 2003;35:1217–1228.
- [17] Lacza Z, Horn TF, Snipes JA, Zhang J, Roychowdhury S, Horvath EM, Figueroa JP, Kollai M, Szabo C, Busija DW. Lack of mitochondrial nitric oxide production in the mouse brain. *J Neurochem* 2004;90:942–951.
- [18] Yvonne Mei Sian Tay AI KSL, Sheu F-S, Jenner A, Whiteman M, Wong KP, Halliwell B. Do Mitochondria make Nitric Oxide? No. *Free Radic Res* 2004;38:591–599.
- [19] Lopez-Figueroa MO, Caamano C, Morano MI, Ronn LC, Akil H, Watson SJ. Direct evidence of nitric oxide presence within mitochondria. *Biochem Biophys Res Commun* 2000;272:129–133.
- [20] Dedkova EN, Ji X, Lipsius SL, Blatter LA. Mitochondrial calcium uptake stimulates nitric oxide production in mitochondria of bovine vascular endothelial cells. *Am J Physiol Cell Physiol* 2004;286:C406–C415.
- [21] Dennis J, Bennett JPJ. Interactions among nitric oxide and Bcl-family proteins after MPP+ exposure of SH-SY5Y neural cells I: MPP+ increases mitochondrial NO and Bax protein. *J Neurosci Res* 2003;72:76–88.
- [22] Yamamoto Y, Henrich M, Snipes RL, Kummer W. Altered production of nitric oxide and reactive oxygen species in rat nodose ganglion neurons during acute hypoxia. *Brain Res* 2003;961:1–9.
- [23] Zanella B, Calonghi N, Pagnotta E, Masotti L, Guarnieri C. Mitochondrial nitric oxide localization in H9c2 cells revealed by confocal microscopy. *Biochem Biophys Res Commun* 2002;290:1010–1014.
- [24] Kojima H, Nakatsubo N, Kikuchi K, Kawahara S, Kirino Y, Nagoshi H, Hirata Y, Nagano T. Detection and imaging of nitric oxide with novel fluorescent indicators: Diaminofluoresceins. *Anal Chem* 1998;70:2446–2453.
- [25] Qi K, Qiu H, Rutherford J, Zhao Y, Nance DM, Orr FW. Direct visualization of nitric oxide release by liver cells after the arrest of metastatic tumor cells in the hepatic microvasculature. *J Surg Res* 2004;119:29–35.
- [26] Lorenz P, Roychowdhury S, Engelmann M, Wolf G, Horn TF. Oxyresveratrol and resveratrol are potent antioxidants and free radical scavengers: Effect on nitrosative and oxidative stress derived from microglial cells. *Nitric Oxide* 2003;9:64–76.
- [27] Kashiwagi S, Kajimura M, Yoshimura Y, Suematsu M. Nonendothelial source of nitric oxide in arterioles but not in venules: Alternative source revealed *in vivo* by diaminofluorescein microfluorography. *Circ Res* 2002;91:e55–e64.
- [28] Roychowdhury S, Luthe A, Keilhoff G, Wolf G, Horn TF. Oxidative stress in glial cultures: Detection by DAF-2 fluorescence used as a tool to measure peroxynitrite rather than nitric oxide. *Glia* 2002;38:103–114.
- [29] Jourdain D. Increased nitric oxide-dependent nitrosylation of 4,5-diaminofluorescein by oxidants: Implications for the measurement of intracellular nitric oxide. *Free Radic Biol Med* 2002;33:676–684.
- [30] Lacza Z, Horvath EM, Pankotai E, Csordas A, Kollai M, Szabo C, Busija DW. The novel red-fluorescent probe DAR-4M measures reactive nitrogen species rather than NO. *J Pharmacol Toxicol Methods* 2005;
- [31] Lacza Z, Snipes JA, Miller AW, Szabo C, Grover G, Busija DW. Heart mitochondria contain functional ATP-dependent K(+) channels. *J Mol Cell Cardiol* 2003;35:1339–1347.
- [32] Broillet M, Randin O, Chatton J. Photoactivation and calcium sensitivity of the fluorescent NO indicator 4,5-diaminofluorescein (DAF-2): Implications for cellular NO imaging. *FEBS Lett* 2001;491:227–232.
- [33] Lacza Z, Snipes JA, Kis B, Szabo C, Grover G, Busija DW. Investigation of the subunit composition and the pharmacology of the mitochondrial ATP-dependent K(+) channel in the brain. *Brain Res* 2003;994:27–36.
- [34] Pacher P, Liaudet L, Bai P, Mabley JG, Kaminski PM, Virag L, Deb A, Szabo E, Ungvari Z, Wolin MS, Groves JT, Szabo C. Potent metalloporphyrin peroxynitrite decomposition catalyst protects against the development of doxorubicin-induced cardiac dysfunction. *Circulation* 2003;107:896–904.
- [35] Kozlov AV, Szalay L, Umar F, Kropik K, Staniek K, Niedermuller H, Bahrami S, Nohl H. Skeletal muscles, heart and lung are the main sources of oxygen radicals in old rats. *Biochim Biophys Acta* 2005;1740:382–389.
- [36] Elfering SL, Sarkela TM, Giulivi C. Biochemistry of mitochondrial nitric-oxide synthase. *J Biol Chem* 2002;277:38079–38086.
- [37] Boveris A, Arnaiz SL, Bustamante J, Alvarez S, Valdez L, Boveris AD, Navarro A. Pharmacological regulation of mitochondrial nitric oxide synthase. *Methods Enzymol* 2002;359:328–339.
- [38] Kanai AJ, Pearce LL, Clemens PR, Birder LA, VanBibber MM, Choi SY, de GWC, Peterson J. Identification of a neuronal nitric oxide synthase in isolated cardiac mitochondria using electrochemical detection. *Proc Natl Acad Sci USA* 2001;98:14126–14131.
- [39] Manzo-Avalos S, Perez-Vazquez V, Ramirez J, Aguilera-Aguirre L, Gonzalez-Hernandez JC, Clemente-Guerrero M, Villalobos-Molina R, Saavedra-Molina A. Regulation of the rate of synthesis of nitric oxide by Mg(2+) and hypoxia. Studies in rat heart mitochondria. *Amino Acids* 2002;22:381–389.
- [40] Gao S, Chen J, Brodsky SV, Huang H, Adler S, Lee JH, Dhadwal N, Cohen-Gould L, Gross SS, Goligorsky MS. Docking of endothelial nitric oxide synthase (eNOS) to the mitochondrial outer membrane: A pentabasic amino acid sequence in the autoinhibitory domain of eNOS targets a proteinase K-cleavable peptide on the cytoplasmic face of mitochondria. *J Biol Chem* 2004;279:15968–15974.
- [41] Henrich M, Hoffmann K, Konig P, Gruss M, Fischbach T, Godecke A, Hempelmann G, Kummer W. Sensory neurons respond to hypoxia with NO production associated with mitochondria. *Mol Cell Neurosci* 2002;20:307–322.
- [42] Kojima H, Urano Y, Kikuchi K, Higuchi T, Hirata Y, Nagano T. Fluorescent indicators for imaging nitric oxide production. *Angew Chem Int Ed Engl* 1999;38:3209–3212.
- [43] Nohl H, Staniek K, Sobhian B, Bahrami S, Redl H, Kozlov AV. Mitochondria recycle nitrite back to the bioregulator nitric monoxide. *Acta Biochim Pol* 2000;47:913–921.
- [44] Artz JD, Thatcher GR. NO release from NO donors and nitrovasodilators: Comparisons between oxyhemoglobin and potentiometric assays. *Chem Res Toxicol* 1998;11:1393–1397.
- [45] Steffen M, Sarkela TM, Gybina AA, Steele TW, Trasseth NJ, Kuehl D, Giulivi C. Metabolism of S-nitrosoglutathione in intact mitochondria. *Biochem J* 2001;356:395–402.
- [46] Chen Z, Zhang J, Stamler JS. Identification of the enzymatic mechanism of nitroglycerin bioactivation. *Proc Natl Acad Sci USA* 2002;99:8306–8311.
- [47] McGuire JJ, Anderson DJ, McDonald BJ, Narayanasami R, Bennett BM. Inhibition of NADPH-cytochrome P450 reductase and glyceryl trinitrate biotransformation by diphenyleneiodonium sulfate. *Biochem Pharmacol* 1998;56:881–893.